THE SOCIETY OF NAVAL ARCHITECTS AND MARINE ENGINEERS
and
THE SHIP STRUCTURE COMMITTEE

Paper presented at the Ship Structures Symposium '93
Sheraton National Hotel, Arlington, Virginia, November 16-17, 1993

Rationally-Based Fatigue Design of Tankers

Owen Hughes[1] and Paul Franklin[2]

[1]Professor of Ocean Structures, Aerospace and Ocean Engineering, Virginia Tech, Blacksburg, Virginia
[2]Graduate Student, Aerospace and Ocean Engineering, Virginia Tech, Blacksburg, Virginia

Abstract

Tanker fatigue cracking has caused concern for the entire marine industry including operators, regulators and classification societies. In response to this concern, various researchers have been developing improved means for evaluating structural fatigue. The authors have developed a practical rationally-based fatigue design method which is sufficiently rapid and efficient to be a part of preliminary structural design. This is important because if fatigue is not adequately addressed at this stage, no amount of detail design will be able to correct or make up for this inadequacy. The method consists of five basic steps: specifying a realistic wave environment, generating a hydrodynamic ship-wave interaction model, computing cyclic nominal stress due to waves and ship motions, using S-N data to predict fatigue life, and using structural optimization to resize the scantlings such that the desired fatigue life is obtained.

The paper describes the method and explains the similarities and the differences with other approaches. Example calculations involving a TAPS tanker are presented which validate the method, and which also demonstrate the importance of both local and overall structure response. The examples show that the heretofore unexplained fatigue cracking of midheight side longitudinals is caused by the local pulsating pressure due to waves and ship motions. This demonstrates clearly that fatigue analysis and design must include response to local panel pressure. Other fatigue analysis methods do not properly account for this effect.

Introduction

Ships operating in various wave climates are subject to cyclic loads beyond those quasi-static or empirical loads normally considered during the design process. In the past, calculation of cyclic loadings has generally been beyond the means of marine designers. However, the current state-of-the-art in numerical methods and relatively affordable computer hardware has eased this limitation.

Background – TAPS Tanker Fatigue

The significance of fatigue cracking in ship structure and the urgent need for adequate fatigue design techniques is illustrated by the problems which have arisen in tankers employed on the TAPS route. In the US Coast Guard's Structural Casualty Study of April 27, 1988 [1] the TAPS tankers were identified as a population of ships with apparently inadequate fatigue resistance. The study reported that during the period 1984 to 1988, 59% of documented structural failures in US flag vessels over 10000 tons occurred in the 13% of the population that served the TAPS route. A close-up investigation of the TAPS tankers [2, 3] reported at least 16 Class 1 fractures (fractures in the oil/watertight boundary or large fractures in other structural members) several of which led to "significant pollution incidences." With respect to the existing state-of-the-art, the Coast Guard report of June, 1990 [2] notes: "Generally, fatigue evaluation is an extremely complex analysis.... Fatigue evaluations are not yet a common and practical component in the design process." The proposed method is aimed squarely at rectifying this situation.

Need for Practical, Rationally-Based, Preliminary Fatigue Design

Traditional rule-based structural design is not valid when considering new and different ship types, and may not be valid when operating conditions for a ship are not in the typical range. Thus there is a need for a rationally-based design method, where the actual anticipated load environment is used to analyze a specific structural design. In recognition of this, the American Bureau of Shipping has recently developed, Liu et al [4], a new (and optional) design procedure, the Dynamic Load Approach (DLA), to be used in conjunction with the Rules.

Further justification for rationally-based design arises when cyclic loading and the resulting fatigue failures are considered. Currently most fatigue control efforts are focused on careful design of connection details and quality control of welds. Such practices are intended to limit the stress concentration factor (SCF) in the region of a connection. However, the stress level at a connection, and thus the resulting fatigue damage, is the product of two quantities: the SCF and the cyclic stress field that is acting in the region of the connection; i.e., the member stress. The stress field (both static and cyclic) is determined by preliminary design which establishes the scantlings of all of the principal structural members. If the preliminary design does not deal adequately with fatigue, the cyclic stress field in the principal structural members will be too large, and no amount of detail design will be able to correct or make up for this inadequacy. Thus there is a paramount need for an efficient method for considering fatigue as a part of preliminary design, and that is the purpose of the proposed method.

In recent years the need has been made even more acute by an increase in the number of fatigue failures due to increased use of high yield steels. Because of the higher static strength of such steels, safety authorities have allowed higher levels of total stress, but this means larger values of cyclic stress as well as static stress. Fatigue strength is separate from yield stress, and in some cases fatigue strength actually decreases with an increase in yield stress. Therefore even though the SCF may be kept at the same value, any increase in the cyclic stress will clearly increase the occurrence of fatigue problems.

Also, as will be shown herein, many of these recent fatigue failures are due, not to simple hull girder bending, but rather to the fluctuating panel pressures acting on the ship hull. However, such pressures can only be obtained by direct calculation and are therefore beyond the capabilities of Rule-based design.

Elements of the Proposed Method

The basic elements of the proposed method for fatigue analysis/design can be reduced to five steps:

1) Specifying a realistic wave environment.

2) Using a hydrodynamic model to calculate the fluctuating panel pressures due to waves and ship motions.

3) Calculating the cyclic nominal stresses due to the ship's structural response (both overall and local) to such pressures.

4) Using S-N data and statistics to assess the fatigue life of the current design.

and for fatigue *design*:

5) Incorporating the fatigue performance as an additional constraint in a structural optimization program, so that the new scantlings will satisfy fatigue requirements, in addition to all other strength requirements.

The first two steps are distinct specialty areas within ocean engineering and have been implemented using recent advances in those specialties. The hydrodynamics model produces a frequency based transfer function relating unit amplitude waves to panel pressures. A rapid and efficient method for whole-ship finite element analysis is then used to convert the transfer function of pressure per unit-amplitude-wave to stress per unit-amplitude-wave. Then each individual wave spectrum, of the set of wave spectra defining the lifetime wave environment, is multiplied by the stress transfer function to calculate a set of response spectra. These response spectra define the lifetime cyclic stress response of the ship, from which the fatigue damage can be calculated. In a design situation, if the fatigue damage is unacceptable, then the optimization process would resize the scantlings so that the cyclic nominal stresses give a satisfactory fatigue life.

This section gives a brief summary of the overall procedure. A more complete development of the method is given in Hughes and Franklin [5].

Wave Environment

The procedures used to establish the TAPS tanker route wave environment are somewhat different from those associated with wave-height *vs.* wave-period scatter diagrams currently contained in oceanographic atlases. The following is a brief review of the methods developed by Buckley [6, 7]. The actual data used for the TAPS example is given in an Appendix to Hughes and Franklin [5].

Long-term wave height spectra measured by NOAA ocean buoys have provided the seaway and wind data used to define two distinct wave climates along the TAPS tanker operating route. The large NOAA data base has been characterized in the following manner. For significant wave height (H_{mo}) class intervals of 1 meter individual wave spectrum energy density ordinates have been averaged to define a single long-term Climatic Wave Spectrum (CWS). The overall analysis procedure uses the CWS as the basic load input.

For computational ease, each CWS has been approximated by an Ochi 3 parameter wave spectrum formulation. In Appendix A of Hughes and Franklin [5], the various wave spectra are thus defined by significant wave height together with the characteristic modal period T_p and spectrum shape parameter λ for the wave climate involved. Given the Ochi (3P) spectrum formulation, the wave energy density is defined as a function of frequency

as required for determination of the response spectrum of interest.

Buckley has performed this procedure for the two generalized wave climates through which the TAPS route passes: West Coast Long Period and Northern High Latitude. Also computed by Buckley from the NOAA buoy data is the probability distributions for wave heading and sea state. For the four NOAA buoys nearest the TAPS tanker route he sorted sustained wind direction data into eight heading sectors. After assuming the wave heading and the direction of the sustained wind were equivalent, the probabilities for various ship headings relative to wave direction were computed. Also for each buoy, the wave data were sorted into 12 class intervals, ranked by severity from H_{m_o} = 0.5 m to 10.0 m, and the probability of occurrence of each wave height was computed.

Hydrodynamics

The hydrodynamic modeling of the interaction between the ship and the seaway is one of the main challenges in any analytical approach for assessing fatigue damage. Currently the common approach towards calculating ship motions and hull girder loading is strip theory. Strip theory is reasonably accurate for calculating cumulative responses such as motions and hull girder forces, but it cannot provide accurate values for pressures acting on local structure.

A recent improvement over strip theory is the linear 3-dimensional hydrodynamic technique. This technique solves the flow problem using a fully 3-dimensional panelized model of the hull, rather than prismatic strips. The solution therefore has increased accuracy, especially for a ship with forward speed. The linearity assumptions are valid for nearly all of a ship's operating conditions and lead to computationally efficient solutions. Linearity assumptions are not accurate during extreme storm conditions, but because of the relative infrequency of these conditions the associated cumulative fatigue damage is relatively small. The great value of linear 3-dimensional theory for this research effort is that it provides panel pressures, which are often crucial to obtaining member cyclic stress to the required degree of accuracy.

Hydrodynamic modeling for the current project is performed using the Small Amplitude Motion Program (SAMP) written by Dr. Woei-Min Lin of SAIC Incorporated. SAMP is a linear 3-dimensional ship motions and loads program. It produces pressure values for individual panels and also calculates hull girder bending moment and shear force. SAMP is thus well suited for fatigue analysis.

Calculation of Transfer Function for Cyclic Stresses

The next step of the analysis procedure is to generate a set of transfer functions, $H^2\,\sigma\,(f_e)$, between a unit amplitude wave at encounter frequency f_e and the cyclic stress level in the member of interest. The individual transfer functions in the set correspond to the various structural load types (hull girder or panel pressures) and tanker operating conditions.

Each specific type of load has its own subset of transfer functions. For the relatively low speed TAPS tankers, the primary loads relating to fatigue are hull girder bending and local wave induced panel pressure fluctuations. Each load based subset of transfer functions has its own subset of transfer functions for every operating condition of the ship. The operating conditions consist of permutations of such variables as ship speed (V_{ship}), heading relative to the waves (Θ), and draft. The service life of the TAPS tankers can be described by the following operating condition variables.

V_{ship} = constant of 15 knots

Draft = either Loaded or Ballast

Θ = Eight 45^o sectors

There are thus 16 distinct operating conditions (and 16 transfer functions) in each load based subset (hull girder and panel pressures) and consequently a total of 32 transfer functions between unit amplitude waves and stress response must be generated. Such transfer functions are computed by using panel pressure output from the hydrodynamic analysis as a load input to a global finite element model of the ship. The proposed method uses the MAESTRO program for this, because it rapidly generates a whole ship model and obtains accurate values of the representative or "field" stresses in all principal structural members (but not hotspot stresses). This procedure correctly accounts for the complex three-dimensional nature of both the loading and the structure, which cannot be accounted for by simple beam theory.

Calculation of Cyclic Stress Response Spectrum

Once the stress transfer function $H^2_\sigma\,(f_w)$ for each principal member has been obtained, the computation of the response spectra $S_\sigma\,(f_e)$ is a relatively simple process. The most important step is to convert both $H^2_\sigma\,(f_w)$ and the wave spectra $S_w(f_w)$ to wave encounter frequency, f_e. The response spectrum is then simply their product.

$$S_\sigma\,(f_e) = H^2_\sigma\,(f_e)\,S_w\,(f_e) \qquad (1)$$

Computation of Fatigue Damage

The response spectra of the previous paragraph have, in general, a Weibull distribution. Known statistical properties of the Weibull distribution can be invoked and combined with the appropriate S-N curves to compute a fatigue damage ratio, η. The fatigue damage ratio is a design oriented measure of fatigue life: a η of 1.0 or larger is a predictor of fatigue failure. The proposed fatigue design method uses the S-N curves of the British Welding Institute [8], which are already used by many ship and offshore structure approval bodies such as the American Bureau of Shipping [9], Det norske Veritas [10] and the UK Department of Energy [11]. The joint classification system associated with these curves empirically includes the stress concentration factor (SCF) which occurs as the result of a welded joint.

As shown in [5], for a Weibull distribution of stress amplitudes the fatigue damage ratio is

$$\eta_{RSP} = \frac{N_{RSP}}{C}\left\{8m_0 \ln\left(\frac{2\sqrt{1-\varepsilon^2}}{1+\sqrt{1-\varepsilon^2}}\,N\right)\right\}^{m/2} \times (\ln N)^{-m/k}\,\Gamma\left(1+\frac{m}{k}\right) \qquad (2)$$

The symbols in the above equation are defined at the end of the paper.

Several studies have shown that peak values of hull girder bending in tankers follow a Weibull distribution with k = 0.7 to 1.0 [12, 13]. Equation (2), with an appropriate value of k, is therefore implemented for the hull girder bending load set.

In contrast, the stress amplitudes due to panel pressure follow the Rayleigh distribution. Panel pressures are due to the sum of many sinusoidal waves and a large number of harmonic ship motions. Therefore from the central limit theorem the panel pressures themselves follow a Gaussian process. It is also reasonable to assume that the fluctuations of panel pressure are narrow banded (cross the mean pressure level between each peak value) and have a mean value close to zero. Consequently the cyclic stresses due to panel pressures also have a Gaussian distribution and a mean value close to zero. For such a process the peak values follow the Rayleigh distribution. This distribution is simply a special form of the Weibull distribution with parameters of k = 2 and $\varepsilon = 0$. Hence for pressure-derived stresses the fatigue damage ratio is

$$\eta_{RSP} = \frac{N_{RSP}}{C}(8m_0)^{m/2}\,\Gamma\left(1+\frac{m}{2}\right) \qquad (3)$$

The total fatigue damage ratio for a particular structural member is the sum of the fatigue damage ratios for each response spectrum. For the purposes of this paper it will be convenient and informative to keep the various loading conditions initially separate and report a distinct damage ratio for each (i.e..., hull girder bending, ηhb, and panel pressure fluctuations, ηpp). In any case, when the total fatigue damage ratio equals or exceeds 1.0, the relevant member is considered to have failed.

Satisfying Fatigue Requirements as a Part of Preliminary Design

The final step in the method is to incorporate the requirement of satisfactory fatigue performance, as measured by the damage ratio, as another of the constraints in an overall structural optimization process. In this way the member scantlings will automatically be resized such that their nominal stresses will give a lifetime damage ratio that satisfies the specific factor of safety against fatigue. Simultaneously, the optimization process also resizes the scantlings so as to satisfy all other design constraints, notably avoiding all structural failures and fulfilling all designer-specified constraints, such as fabrication requirements.

This optimization process, and also a whole-ship finite element analysis and a rigorously thorough failure analysis (examining all failure types for all members) already exist in the form of the MAESTRO computer program for preliminary structural design. It is a proven technology, having been used by many designers for many years. Its design method can be summarized as follows:

1) For every possible failure mode, and for all members and load cases, calculate the current load effects, Q (stresses etc.) and the corresponding failure (or other limit) values of those load effects, Q_L.

2) Set up a mathematical optimization problem in which the constraints are $\gamma Q \le Q_L$, where $d\gamma$ is the product of any number of "partial" safety factors, each of which accounts for the probabilities of the various loads and failure modes, the degree of seriousness of the latter, and the various uncertainties (especially in predictions).

3) For any designer-specified measure of merit, such as a nondimensional combination of cost and weight, solve the optimization problem using dual level sequential linear programming.

It should be noted that we are here dealing only with preliminary design, the purpose of which is to obtain satisfactory nominal cyclic stresses. The fatigue analysis presumes certain types of structural details and degrees of weld quality. Therefore it is still necessary that the detail design should pay careful attention to both of these all-important aspects of fatigue design.

Comparison with Other Methods

David Taylor Research Center

Approximately a decade ago Sikora et al (14) outlined a procedure in use at DTRC for performing fatigue analysis of ships. Their paper uses experimentally and empirically derived transfer functions to relate hull girder bending moment to unit amplitude waves. The transfer functions are then multiplied by known wave spectra to compute a series of bending moment response spectra and their respective probability density functions. From the probability density functions a histogram of cyclic stress amplitude *vs.* the number of cycles for which the stress value is exceeded was created. Sikora et al then demonstrated how to directly apply the Palmgren-Miner cumulative fatigue damage theory to the histogram in order to compute fatigue life.

The fatigue analysis presented here differs from the approach of Sikora et al. in four significant areas. First of all, physical modeling and extensive tank testing of the ship are not required. Secondly, the analysis is not limited to overall ship quantities such as hull girder bending. Thirdly, several well known statistical procedures can be implemented to streamline and improve the fatigue damage calculation. Finally, a specific set of widely available S-N curves is incorporated.

American Petroleum Institute

A second existing source of guidance for analyzing fatigue in ocean structures is the American Petroleum Institute (API), which devotes a chapter in its RP-2A [15] to fatigue analysis. The API RP-2A outlines a basic fatigue method for offshore structures. The technique includes recommendations for the wave climate description, dynamic modeling of the structure, development of the stress transfer function and calculation of the fatigue damage ratio. The API recommendations are limited in generality; they consider only open-framed platforms consisting of tubular members. The recommendations are also limited in scope; [15] is a publication of recommended practices and does not specify analysis procedures in detail.

Structural Maintenance Project

Very recently a Joint Industry Project titled the Structural Maintenance Project or SMP, based at the University of California at Berkeley, published a series of volumes entitled *Structural Maintenance for New and Existing Ships* [16]. The Berkeley SMP, as the name implies, is a broadly based study on the structural maintenance of existing ships. Under this maintenance theme it addresses corrosion, fatigue, structural monitoring and repair management. Its fatigue analysis method differs from those previously mentioned in that it is mainly intended for the analysis of existing ships rather than the design of new ships.

For this same reason, the method presented herein also differs from that of the SMP. The most significant differences between the two projects are:

1) SMP uses less precise wave data, based on Marsden squares, whereas for the TAPS tankers we use the more accurate climatic data from the NOAA wave buoys located directly along the TAPS route.

2) For hydrodynamic analysis SMP uses strip theory instead of a 3-D panel method.

3) SMP uses local FE analysis of specific joints and corresponding hotspot stresses in the fatigue analysis, in conjunction with either hotspot S-N curves or fracture mechanics for failure criteria. In contrast, our method uses the aforementioned joint classification system and S-N curves.

4) The tankers studied by SMP did not include any which had extensive cracking of side longitudinals at the midheight of the ship.

The first difference is primarily an issue of availability. The improved wave data from NOAA buoys and the work Buckley has done to convert the raw data into a usable engineering format is quite recent and is not yet widely available. Even when published, Buckley's data will be limited to those ocean areas for which NOAA buoy data exists (primarily North American coastal waters). Unfortunately the wave directionality for the published Marsden squares data is not sufficiently differentiated by wave height to correctly allow for specific trade routes.

The second difference may also be considered an issue of availability. Efficient 3-D panel based hydrodynamic programs, while certainly a large improvement over strip methods, are relatively new. Indeed the early version of SAMP which was used for the calculations in this report did not have an allowance for roll damping. Future calculations will be performed using the current version of SAMP, which does include roll damping and several other improvements to streamline calculations.

The use of local FE analysis on specific joints is an important step in analyzing existing structure, especially when concerns of continued crack growth arise. However such a process is computationally quite intense and is, as of yet, still too cumbersome for design techniques.

Similarly, failure criteria consisting of hotspot S-N curves or fracture mechanics are appropriate for analyzing existing, problematic structure, but have drawbacks in terms of a design method. One of the largest difficulties with hotspot S-N curves is that no widely accepted collection appears to exist. The SMP team conceded as much when they took non-hotspot curves and scaled them according to engineering judgment. As for fracture mechanics, this

is again a rather complicated analysis best suited for examining known problem areas.

Finally, when it came to performing specific example calculations, SMP chose to analyze a group of ships which did not contain a large number of documented failures of the midheight side longitudinals. As such, a comparison of the relative importance of panel pressures and hull girder bending stress was not a subject in the SMP study.

American Bureau of Shipping

ABS has recently published a design document *Guide for the Fatigue Strength Assessment of Tankers* (9), which sets forth a simplified method for fatigue assessment. The *Guide* implicitly includes the same basic elements as the fatigue analysis methods described above; the scope of these implicit elements is summarized in the *Guide's* preface, "... considered in the derivation of the criteria are: the Palmgren-Miner linear damage model, S-N curve methodologies, a long term sea environment representative of the North Atlantic Ocean (which is to be considered for unrestricted service classification), and a nominal vessel service life of 20 years." However, because the derivation of the *Guide* simplifies, condenses and combines these elements, it also limits the fatigue assessment in terms of both accuracy and flexibility. The *Guide* addresses this concern and recommends that more elaborate analysis methods are required in cases where the applicability of the derivation is in question.

At the 1992 SNAME annual meeting Liu et al [4] presented a paper describing ABS's Dynamic Load Approach, including a case study involving a more rigorous fatigue analysis than that of the *Guide*. Although the fatigue calculations of the case study are only briefly described, they appear to be essentially the same as the first four steps of our method: wave data (in this case observational wave data from the North Atlantic), a hydrodynamic motion and loads analysis, finite element analysis to obtain stress transfer functions, and S-N data plus long-term statistics to calculate lifetime fatigue damage. However there are two aspects in which we believe our method is more accurate: the wave data and the treatment of cyclic stress due to local panel response.

The Walden wave data used in the ABS case study is based on weather ship observations from two specific weather stations. ABS did not attempt to model the actual operating environment for the tanker studied, but simply used data from an extreme environment in the North Atlantic. Thus for two reasons the authors prefer Buckley's wave data over Walden's: they have greater confidence in wave data derived from NOAA buoy measurements than strictly observational data, and Buckley's wave data permits the analysis to use the actual lifetime wave environment of the TAPS tankers.

As for the computation of the stress transfer function, Liu et al [4] used the midship vertical bending moment (VBM) to characterize the peak value, the shape and the statistics of the frequency response function for all types of stress and for all of the structural members studied. While this simplifies the computation, such an approach is not valid for those structural responses not dominated by VBM or for members far from midships.

Most of the structural members in a ship's hull incur two types of cyclic stress: one due to hull girder bending and one due to direct response to the local cyclic pressures due to wave and ship motions. This paper contains three findings regarding these two stress types:

1) In some regions of the hull the local pressure induced stresses contribute significantly to, and even dominate, fatigue accumulation.

2) Example 2 (Figures 8 and 11) will show that the transfer functions of these two stress types have very different shapes.

3) The statistical properties of the two stress distributions are also different, as was shown in equations 2 and 3.

In the ABS method these two types of stress are combined and are processed together. The third step of their method has two levels: a whole-ship finite element analysis using a wave load corresponding to the frequency of the peak value of the midship VBM transfer function, and local fine mesh analyses. The combining of the stress types occurs when local pressures and nodal displacements from the whole-ship analysis are applied to the fine mesh models to generate a corresponding peak value of the member stress. The transfer function for the combined stress is then constructed by assuming that it has the same shape as the transfer function for the midship VBM. Then in the fourth step, since the stresses have been combined, the pressure-induced stress is treated as if it had the same statistical properties as the hull girder stress.

Nevertheless, in the four basic steps that constitute fatigue *analysis*, the ABS method and the method presented herein share the same philosophy and approach. The distinction is that our method also provides for fatigue *design*; it has a fifth step in which the results of the fatigue analysis become additional constraints in a structural optimization process, in which the member scantlings are resized such that their nominal cyclic stresses give a satisfactory fatigue performance, while also satisfying all other constraints. In fact, we believe that optimization is crucial for this approach to fatigue because it not only guides, but also automates the entire process. Without it the process takes on a trial and error nature and becomes

so tedious and lengthy that it could not be done within the cost and time constraints of preliminary design.

Discussion of TAPS Fatigue

Before demonstrating the fatigue analysis method, we will step back and look at the trends which have developed in the fracture data for one class of ship. The USCG report of May 1991 [3] reported that the Atigun Pass class was subject to fractures in both the side longitudinals and in the bottom longitudinals (in way of limber holes). For this study we examined a summary, prepared for the USCG, of the side longitudinal fractures in one of the Atigun Pass tankers. The graphical representation of this data, Figures 1 and 2, may at first seem rather inexplicable, but actually the fractures occur mainly in patterns for which good engineering reasons can be presented.

Until now fatigue in longitudinal members has been customarily associated with the cyclic stresses due to hull girder bending. Hence the most intriguing anomaly in the data, which has not heretofore been adequately explained, is that some (indeed many) of the cracks are located at or near the ship's neutral axis. Since hull girder bending stresses are negligible at such a location, there must be some other significant cause or source of fatigue damage. It will be shown (in Example 3) that the cause of this cracking is the pulsating hydrodynamic pressure on the ship's hull due to waves and ship motions.

A second anomaly is the large difference in the number of side longitudinal fractures between the port side (210) and the starboard side (296). This has frequently been attributed to the direction of travel during cargo and ballast voyages. The weatherside (exposed to seas from the west) during the more heavily loaded cargo voyage is the starboard side of the ship. While this is correct, we would like to offer a more complete explanation.

During cargo voyages the waterline of the Atigun Pass tankers is approximately at longitudinal 44. Such waterline longitudinals are most heavily affected by local pulsating pressures. Conversely in a ballast voyage these same tankers ride approximately 15 feet higher in the water. The waterline is then in the vicinity of longitudinal 38. The higher longitudinals on the port side are therefore subject to less pulsating pressure. The data reflects this reality with a strong grouping of fractures on the starboard side from longitudinals 39 to 45. Using similar logic it might be expected to see a grouping of fractures on the port side from longitudinals 34 to 40. This however does not occur, and the reason is that such longitudinals are larger, having been sized in proportion to the hydrostatic load, and consequently they have smaller fluctuating stress values. This shows, incidentally, that the customary linear sizing of longitudinals based purely on the hydrostatic load is not appropriate because it does not meet the requirements of the hydrodynamic loading.

When looking at the same starboard side data a third pattern appears which again at first seems to be an anomaly. Longitudinals 41, 44 and even 46 are within the high risk zone and indeed have a poor fracture history at transverse bulkheads, but are remarkably free of fractures at other frames. The explanation for this phenomenon is found by comparing the connection detail between longitudinal 44 and a web frame, Figure 3, with a typical longitudinal to web frame detail, Figure 4, and finally the typical longitudinal to transverse bulkhead detail, Figure 5.

It is apparent that the large brackets used in L41, L44 and L46 (Figure 3), reduce the susceptibility of these longitudinals to fatigue. These large brackets have been credited as being both an improved fatigue design detail ("softening" the SCF) and with shortening the effective span (and thus reducing stress levels at the connection). But a more complete and convincing explanation can be obtained by examining the bending moment distribution in a typical side longitudinal segment between transverse frames, which is that of a clamped beam as shown in Figure 6. The bending moment and thus stress at the end of the bracket, the location most likely to generate a fatigue fracture, is almost exactly zero and therefore little or no fatigue damage will occur. We would like to suggest that this very beneficial geometric arrangement should be used wherever possible in structural design. In contrast, the smaller brackets used in the details shown in Figures 4 and 5 have their edges, and thus the SCF, at locations of much higher bending stress. These smaller brackets are therefore much more susceptible to fatigue damage.

It is worth noting that all of the patterns discussed herein require consideration of fluctuating panel pressures. Any design or analysis technique which ignores panel pressures would fail to predict neutral axis fatigue cracking, a starboard/port fatigue difference or a differentiation between the bracket connections. Similarly, any technique which treats the local pressure-induced stress in the same manner as hull girder stress would not be able to correctly assess or quantify these three phenomena.

In the following section we will present four example analyses in order to quantify some of these fracture patterns. The example calculations will look at both panel pressure fluctuations for side shell longitudinals and hull girder bending stresses for the lower longitudinals and the bottom shell structure. Due to time and funding constraints the example calculations are not comprehensive, but they serve to illustrate the proposed analysis method and demonstrate its capabilities.

Example Calculations

The four example calculations presented herein are based on an Atigun Pass class tanker operating on the TAPS route. The analyses are limited to only one buoy location (out of four; hence corresponding to 1/4 of the ship's voyage life) and only one operating condition (out of 16: 8 headings and 2 loading conditions). A complete analysis would therefore repeat the following procedures a total of 64 times.

The following data, describing a February 1992 voyage from Valdez to San Francisco will be used for all example calculations [17].

V_{ship} = 15 knots

Draft = 50 ft

Light Ship = 24707 LT

Displacement = 168956 LT

L_{cg} (from A.P.) = 456.16 ft

V_{cg} (above keel) = 40.73 ft

Example 1: Panel Pressure, Lower Side Longitudinal (L32)

Longitudinal 32 is in the lower side shell approximately 163" above the bilge. Because longitudinal 32 is in the side shell and at a significant distance from the hull's neutral axis, it is reasonable to expect fatigue damage due to both panel pressure fluctuations and hull girder bending. We examine the welded joint between the outer edge of the web of the side longitudinal and the flat bar bracket at a typical web frame (see Figure 4). The first example calculation computes the contribution of local pressure fluctuations to fatigue damage. Example 2 will examine fatigue damage due to hull girder bending at this same location. Since the purpose is simply to illustrate the method, both calculations are done for only one heading.

Pressure Transfer Function

A single transfer function, $H^2(f_e)$, is required for this calculation. Due to the energy content of the wave environment a transfer function throughout the range, $f_w = 0.04$ to 0.15 Hz is sufficient. The panel geometry used for the hydrodynamic analysis uses 165 panels to describe the submerged portion of the hull. The panel identified as Surface 5, Station 6, Waterline 3, encompasses the location of longitudinal 32 and frame 54. Time histories of panel pressures are calculated for a series of regular waves using the linear hydrodynamics program SAMP. The SAMP runs use the following parameters:

f_w = 0.04,0.06,0.1,0.15 Hz

Wave Amplitude = 390 in

From each time history (see Hughes and Franklin (5)) the amplitude of the steady state pressure fluctuation for the panel of interest is extracted and the quantity

$$\left(\frac{P_{amp}}{Wave_{amp}}\right)^2$$

is plotted against wave frequency. The result is Figure 7, a transfer function for panel pressure.

Stress Transfer Function

For the relatively low frequency pressure fluctuations normally considered, a static stress analysis is sufficient. The overall fatigue analysis method proposed herein normally uses MAESTRO on a PC or workstation to rapidly generate a whole ship structural model, and obtain representative or "field" stresses in all principal structural members (but not hotspot stresses). This enables the analyst to accurately assess member field stresses for a given load with the assurance that the local boundary conditions are complete and correct. However, even this simple PC-based analysis was not required for the side longitudinals considered herein, because each segment between transverse frames is nothing more than a clamped beam subjected to a uniform distributed load. Therefore, stress levels in the outer edge of the web were calculated using beam theory, allowing for the asymmetry of the flange. The resulting transfer function

$$\left(\frac{\sigma_{amp}}{Wave_{amp}}\right)^2$$

is given by Figure 8.

The steep decay of Figures 7 and 8 is primarily due to the frequency dependence of the pressure values within an ocean wave. The pressure distribution with depth, p(y), for an undisturbed linear wave is given as

$$p(y) = \rho g a \exp\left(\frac{\omega^2 y}{g}\right)\sin(\omega t)$$

Therefore, especially for higher frequency waves, there is a substantial decay in pressure at a depth y beneath the mean water line.

Wave Spectrum

The TAPS Tanker route and the location of the four buoys which have been chosen to describe the wave environment are shown in Figure A-1 of Appendix A of Hughes and Franklin [5]. The length of the route defined by each buoy was scaled from the map and divided by total route length to compute the location probabilities in Table 1.

Buoy	P(loc)
46001	0.32
46004	0.26
46005	0.14
46002	0.28

Table 1
Location Probability

The wave spectra for the buoys are calculated based on the Ochi parameters given in Appendix A [5]. Shown in Figure 9 are both the wave and encounter frequency spectra for Buoy 46002 at H_{m_o} = 4.0 m. Such an overlaid plot demonstrates the importance of the encounter frequency modification.

Response Spectrum

For each sea state of concern, H_{m_o} = 1.0 to 13.0 m, the transfer function H_σ^2 is multiplied by the respective wave spectrum $S_w(f_e)$. The spectral moments, m_0 and m_2, of the resulting response spectrum $S_\sigma(f_e)$ are then calculated. As an illustration of the intermediate results a single response spectrum is given in Figure 10.

Damage Ratio

The damage ratio, η, is calculated by combining the response spectral moment, m_0 with the parameters C and m (which describe a S-N curve) in Equation (16). The values of C and m are based on the joint classification system of the Welding Institute [8]. For the bracketed end connection of the side shell longitudinals to the transverse web frame, Figure 4, the joint type is 4.2 and the classification is G. The S-N curve parameters are thus, C = 1.738×10^{18} and m = 3.0. The operating lifetime used in the example is T_{life} = 20 years and the probability associated with each response spectra is calculated in Table 2.

The response spectrum probabilities of Table 2, the spectral moments and the fatigue strength parameters are all combined to compute the fatigue damage ratio of a single spectrum. Table 3 shows the contribution to η for 11 different sea states and for each of the example calculations performed in this section. Each contribution represents only the damage accumulated during a single sea state, location, draft, heading and speed combination.

Example 2: Hull Girder Bending, Lower Side Longitudinal (L32)

This example demonstrates the technique used to calculate fatigue damage due to hull girder bending at the same location as in Example 1. The resulting damage can thus be algebraically added to the results from the panel pressure analysis. The operating condition for this example is again: loaded, forward speed of 15 knots and head seas. The wave spectra are also identical. The transfer function for this particular operating condition is given in Figure 11.

To demonstrate the difference between hull girder and panel pressure response, we examine Figures 8 and 11 which give the frequency response transfer function of stress in a side shell longitudinal due to both. The stress transfer function for VBM has a distinct peak which is a result of the hull's response to the integration of many

H_{m_0}	P(V_{ship})	P(Θ)	P(Draft)	P(H_{m_0})	P(loc)	P(RSP)
1.0	1.0	.055	0.5	.1905	.28	1.47×10^{-3}
2.0	1.0	.0615	0.5	.3171	.28	2.73×10^{-3}
3.0	1.0	.1055	0.5	.2323	.28	3.43×10^{-3}
4.0	1.0	.123	0.5	.1455	.28	2.51×10^{-3}
5.0	1.0	.1005	0.5	.0667	.28	9.39×10^{-4}
6.0	1.0	.0925	0.5	.0278	.28	3.60×10^{-4}
7.0	1.0	.099	0.5	.0113	.28	1.57×10^{-4}
8.0	1.0	.077	0.5	.0042	.28	4.53×10^{-5}
9.0	1.0	.056	0.5	.0028	.28	2.20×10^{-5}
10.0	1.0	0.00	0.5	.0007	.28	0.0
>10.0	1.0	0.00	0.5	.0007	.28	0.0

Table 2
Response Spectra Probabilities for Buoy 46002, Θ = 180 and Draft = 600 in

H_{m_0}	η				
	L32 Panel Pressure	L23 Hull Girder	L43 Panel Pressure	Bottom Longitudinal†	Bottom Longitudinal‡
1.0	4.59×10^{-6}	2.43×10^{-6}	6.25×10^{-4}	3.68×10^{-5}	1.01×10^{-5}
2.0	1.08×10^{-4}	7.22×10^{-5}	1.06×10^{-2}	1.09×10^{-3}	2.99×10^{-4}
3.0	1.84×10^{-4}	1.64×10^{-4}	1.01×10^{-2}	2.48×10^{-3}	6.79×10^{-4}
4.0	4.56×10^{-4}	4.61×10^{-4}	1.91×10^{-2}	6.98×10^{-3}	1.91×10^{-3}
5.0	4.29×10^{-4}	4.52×10^{-4}	1.47×10^{-2}	6.84×10^{-3}	1.87×10^{-3}
6.0	3.4×10^{-4}	3.59×10^{-4}	1.01×10^{-2}	5.44×10^{-3}	1.49×10^{-3}
7.0	2.72×10^{-4}	2.82×10^{-4}	7.11×10^{-3}	4.27×10^{-3}	1.17×10^{-3}
8.0	1.32×10^{-4}	1.33×10^{-4}	3.11×10^{-3}	2.01×10^{-3}	5.49×10^{-4}
9.0	9.93×10^{-5}	9.66×10^{-5}	2.16×10^{-3}	1.46×10^{-3}	4.00×10^{-4}
10.0	0.00				
>10.0	0.00				
Total	2.03×10^{-3}	2.02×10^{-3}	7.75×10^{-2}	3.06×10^{-2}	8.37×10^{-3}

Table 3
Fatigue Damage Ratios for Buoy 46002, Θ = 180 and Draft = 600 in
† Basic Drain Hole
‡ In way of Butt-Weld

panel pressures distributed over the entire hull. In contrast the transfer function for the localized response to panel pressure fluctuation is dominated by the pressure distribution within the incident wave. Because the basic nature and shape of the two transfer function are quite different, it is impossible to accurately derive the function for panel pressure by scaling the function for midship VBM.

As in Example 1, the joint type is 4.2, the class is G and the S-N curve parameters are: $C = 1.738 \times 10^{18}$ and $m = 3.0$. The fatigue damage ratio for each sea state is summarized in Table 3. Again the total from Table 3 represents the contribution to the fatigue damage ratio due to hull girder bending for a single operating condition and a single buoy location. A complete analysis would proceed to evaluate all other operating headings as well as each buoy location, but as explained earlier, it is not yet possible to obtain results for all headings.

Example 3: Panel Pressure, Midheight Side Longitudinal (L43)

Longitudinal 43 is located approximately at the ship's design water line and thus panel pressures do not decay as quickly, in comparison to longitudinal 32, with wave frequency. Therefore the frequency range of the analysis must extend beyond the earlier example. It should also be noted that longitudinal 43 is designed for a smaller hydrostatic head than longitudinal 32 and accordingly a smaller cross sectional area is used. The result is higher stresses in longitudinal 43 for equivalent panel pressures. Figure 12 shows the encounter frequency transfer function of outer web stress for both longitudinals 32 and 43.

The stress value for longitudinal 32 starts at a relatively low value and decays to an insignificant quantity within the frequency range of significant wave energy. The transfer function for longitudinal 43 however, starts at a large value and remains significant throughout the frequency range. The fatigue analysis for longitudinal 43 is performed in an identical manner to that shown for longitudinal 32. The joint type and class are again 4.2 and G respectively. The pertinent data for the calculation is given in Table 3.

The final result of Table 3 is a damage ratio of 0.078, or more than 75 times the damage due to pressure in longitudinal 32 for the same operating condition. This value is for 1 out of 64 lifetime operating conditions and therefore represents a significant contribution towards a possible fatigue failure. For both longitudinals 32 and 43 other headings involve much more rolling, and rolling can typically increase the time-varying dynamic component of pressure on a ship's side by a factor of two or more, depending on the degree of rolling. Thus for the full set of operating conditions the value of 0.078 will be magnified not just by 64 but more likely by some value between

100 and 150, and possibly even larger. If it is 100 then the lifetime (20 year) fatigue damage ratio becomes 7.8, which means a crack would appear in only 20/7.8 = 2.6 operating or approximately 4 calendar years*. This agrees very well with the actual fatigue cracking history of the example ship, and thus provides good validation of the proposed method.

It is also important to note that longitudinal 43 is near the ship's neutral axis. Any analysis procedure which relies exclusively on hull girder bending would predict little or no fatigue damage to such a member. This example shows that fatigue damage due to panel pressures can be quite significant, and that fatigue analysis must consider the dynamic panel pressures due to waves and ship motions, including roll.

Example 4: Bottom Longitudinal; Web to Plating Weld

The bottom longitudinals of the TAPS tankers have also been subject to fatigue cracking. Such cracks have tended to occur in the region of drain holes in the longitudinals, as shown in Figure 13. There are two types of drain holes, as shown in Figure 14.

The basic drain hole is an oval cut-out. The oval maintains the continuity of the web-to-plating weld (joint type 4.1b, weld class F2), but creates a stress concentration factor of approximately 2.0 at the longitudinal weld. In the way of erection butt welds the oval is interrupted, leaving a gap in the longitudinal weld. The gap eliminates the SCF in the web plating, but degrades the joint type to 4.2, weld class G.

For bottom structure hull girder bending stresses are large. In contrast the wave-induced pressures have attenuated to a quite small value and therefore the cyclic stresses due to local panel response are also small and do not contribute to fatigue.

Example 4a: Basic Drain Hole

The stress transfer function for a bottom longitudinal in the region of a basic drain hole is given in Figure 15. Table 3 summarizes the fatigue damage ratio calculation.

Example 4b: Erection Butt-Weld Drain Hole

Again the stress transfer function is given in Figure 16 and a summary of the fatigue damage ratio calculation is again given in Table 3.

Results Summary and Conclusions

Summary

The examples shown above are summarized in Table 4. The relative importance of local panel pressures and overall hull girder bending is shown for three different member types. One of the most important results of these analyses is to show the importance of local panel pressures in fatigue analysis.

Examples 1 and 2, which consider a typical longitudinal approximately 163" above the bilge, report nearly identical fatigue damage due to panel pressure and hull girder bending. Therefore any analysis that only examines hull girder bending would dangerously overestimate the fatigue life by a factor of two.

Example 3 continues the theme by considering a longitudinal at or near the ship's neutral axis. Although a hull girder analysis would indicate no fatigue damage, the panel pressure calculation reveals that such a longitudinal is actually highly susceptible to fatigue damage.

The final examples, 4a and 4b, are the opposite of Example 3. Here panel pressures are not significant, but hull girder bending results in high fatigue damage ratios. The much higher damage ratio for case 4a *vs.* case 4b is due to the SCF of 2.0 used for the basic drain hole.

Conclusions

This report presents a rationally-based method for the fatigue design of ship hulls, which is essentially a synthesis of existing (and proven) analysis tools. The report gives four example calculations for the TAPS tankers which demonstrate the method's practicality and suitability for design. The quantitative results are in excellent agreement with the actual fatigue cracking history for these ships, thus validating the accuracy of the method.

The results also indicate that the heretofore unexplained cracking in the midheight side longitudinals is caused by the pulsating hydrodynamic pressure on the ship's hull due to waves and ship motions. The proposed method was able to achieve this result because it is based on first principles; i.e. direct analysis/calculation of all of the important factors regarding ship hull fatigue. It is also worth noting the practicality of the method: all of the computations required for these examples were performed on a desktop computer.

The examples presented herein are incomplete because they are performed for only a small portion of the ship's

* The value for calendar years is based on a typical value for such tankers of spending 60% of a year at sea. In this case: 2.6/0.6 = 4.3 years.

Example	Member	Analysis	Location within Longitudinal's Web	Damage Ratio†
1	L32	Panel Pressure	At bracket butt weld (Fig 3)	2.03×10^{-3}
2	L32	Hull Girder	At bracket butt weld (Fig 3)	2.02×10^{-3}
3	L43	Panel Pressure	At bracket butt weld (Fig 3)	7.75×10^{-2}
4a	BL	Hull Girder	Below drain hole @ web/plating weld (Fig 13)	3.06×10^{-2}
4b	BL	Hull Girder	Edge of drain hole gap @ web/plating weld (Fig 13)	8.37×10^{-3}

†Damage ratio was calculated for 1/64 of the ship's operating life. A complete analysis would require repeating the process for all combinations of 2 load conditions, 8 headings and 4 buoy locations.

Table 4
Summary of Examples

operating life. Nevertheless they demonstrate conclusively that a meaningful fatigue analysis requires accurate modeling of all load types and major segments of a ship's operating life. Above all, panel pressures must be included in any methodology to examine fatigue of a ship's shell structure. To accurately predict such fluctuating panel pressures requires a 3-D panel-based hydrodynamic analysis, including roll motions. Therefore the proposed method will utilize the now available version of SAMP which includes roll damping and thus accurate values of roll motion.

Acknowledgments

The authors are grateful to SNAME and the Ship Structure Committee for their support of this work. We also wish to thank Mr. Alexander Delli Paoli of Exxon Company, International for providing the data needed to validate the method and demonstrate its practicality.

Symbols

$H^2\,\sigma\,(f)$	Transfer Function of stress per unit amplitude wave
f_w	Wave frequency
f_e	Wave encounter frequency
V_{ship}	Ship velocity
Θ	Ship heading
$s_\sigma\,(f)$	Stress response spectra
$S_w(f)$	Wave spectra
η_{RSP}	fatigue damage ratio for a particular stress response spectra
C	log(C) is the intercept of the cycles axis of the S-N curve
m_0	Zeroth order spectral moment of stress response
m_2	Second order spectral moment of stress response
ε	Bandwidth parameter defined in terms of spectral moments
N	Lifetime number of stress cycles (usually 10^8)
m	Negative slope of the S-N curve
k	Weibull parameter
$\Gamma\,(\,)$	Gamma function
N_{RSP}	Number of lifetime stress cycles for each response spectrum
p_{amp}	Amplitude of cyclic pressure
σ_{amp}	Amplitude of cyclic stress
ρ	Mass density of sea water
a	Wave amplitude
g	Acceleration due to gravity
ω	wave frequency in radians/sec
H_{mo}	significant wave height

References

1. Structural Casualty Study, United States Coast Guard, April 27, 1988.
2. Report on the Trans-Alaska Pipeline Service (TAPS) Tanker Structural Failure Study, United States Coast Guard Report, June 25, 1990.
3. Trans-Alaska Pipeline Service (TAPS) Tanker Structural Failure Study, Follow-up Report, United States Coast Guard Report, May 1991.
4. Liu, D., Spencer, J., Itoh, T., and Shigematsu, K., "Dynamic Load Approach in Tanker Design," Trans. SNAME, 1992.
5. Hughes, O., and Franklin, P., Definition and Validation of a Practical Rationally-Based Method for the Fatigue Analysis and Design of Ship Hulls, SNAME T&R Report No. R-41, February 1993.
6. Buckley, W.H., "The Determination of Ship Loads and Motions: A Recommended Engineering Approach," Naval Engineers Journal, May 1990.
7. Buckley, W.H., "Design Wave Climates for the World Wide Operation of Ships, Part I: Establishment of Design Wave Climates," now in final review.
8. Welding Institute Research Bulletin, 17 (5), May 1976.
9. Guide for the Fatigue Strength Assessment of Tankers, American Bureau of Shipping, New York, NY, 1992.
10. Rules for Design, Construction and Installation of Offshore Structures, Det norske Veritas, Hovik, Norway, 1977.
11. Offshore Installations: Guidance on Design and Construction, U.K. Department of Energy, London, 1981.
12. Little, R.S., Lewis, E.V., and Bailey, F.C., "A Statistical Study of Wave Induced Bending Moments of Large Oceangoing Tankers and Bulk Carriers," Trans. SNAME, 1971.
13. Lewis, E.V., and Zubaly, R.B., "Dynamic Loadings Due to Wave and Ship Motions," STAR Symposium, SNAME, 1975.
14. Sikora, J., A. Dinsenbacher, and J. Beach, "A Method for Estimating Lifetime Loads and Fatigue Lives for Swath and Conventional Ships," Naval Engineers Journal, May 1983.
15. Recommended Practice for Planning, Designing and Constructing Fixed Offshore Platforms, 19th Edition, (API RP-2A), American Petroleum Institute, August 1, 1991.
16. Structural Maintenance for New and Existing Ships, Reports SMP-1-5 through 5-1, Department of Naval Architecture and Offshore Engineering, University of California at Berkeley, September 1992.
17. Data provided by Exxon Shipping Co., through A. Delli Paoli of Exxon International.

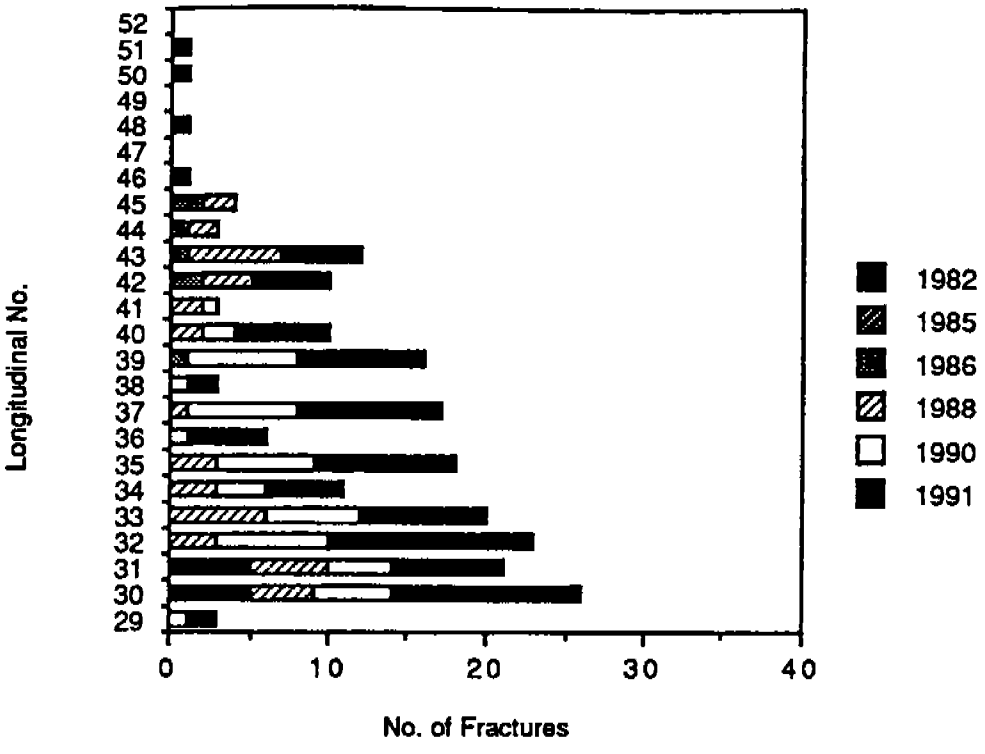

Figure 1
Vertical Distribution of Cracks, Port Side Longitudinals

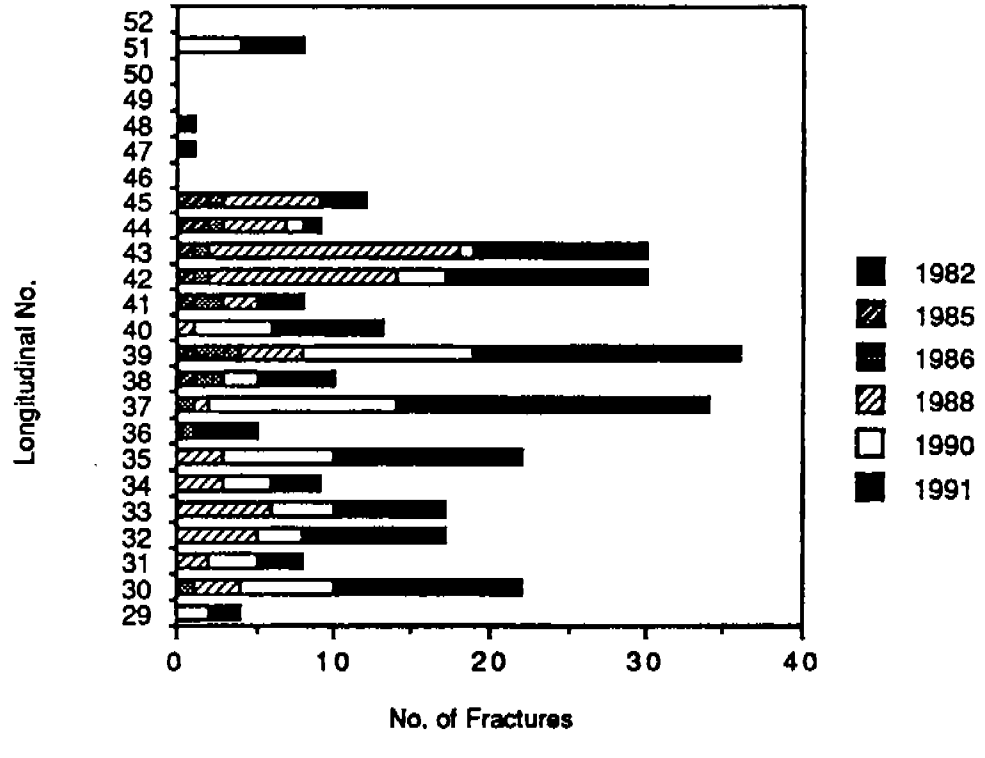

Figure 2
Vertical Distribution of Cracks, Stbd. Side Longitudinals

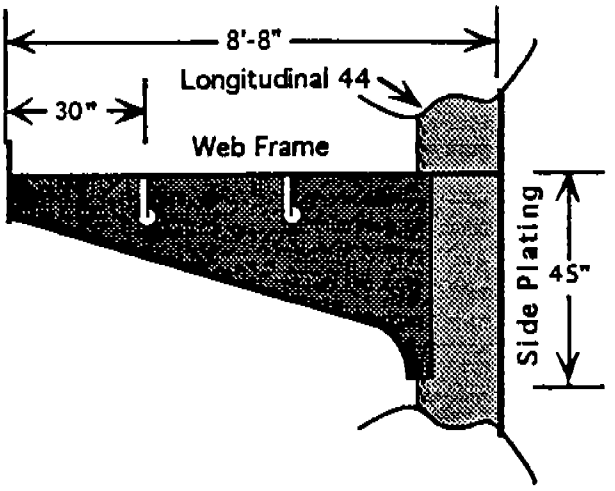

Figure 3
Longitudinal 41, 44 and 46 at a Web Frame

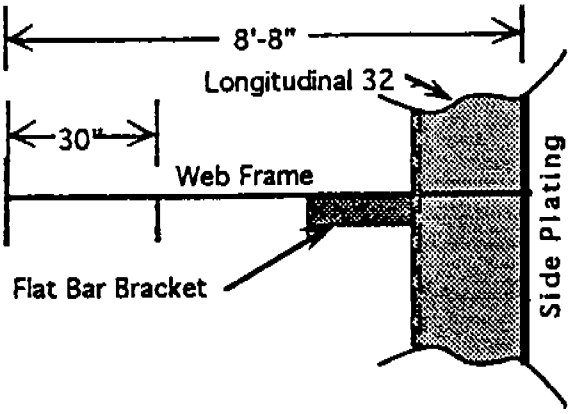

Figure 4
Typical Longitudinal at Web Frame

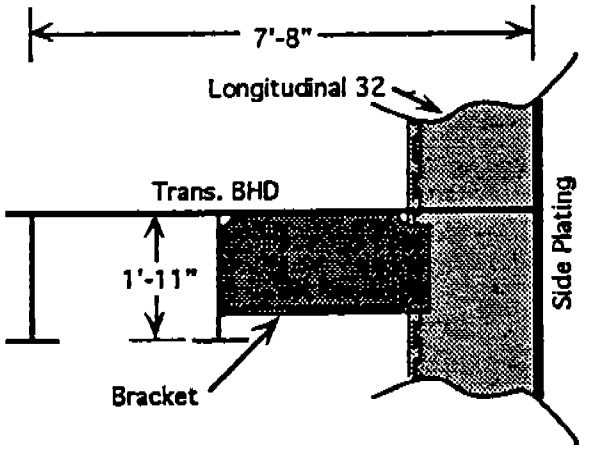

Figure 5
Typical Longitudinal at Transverse Bulkhead

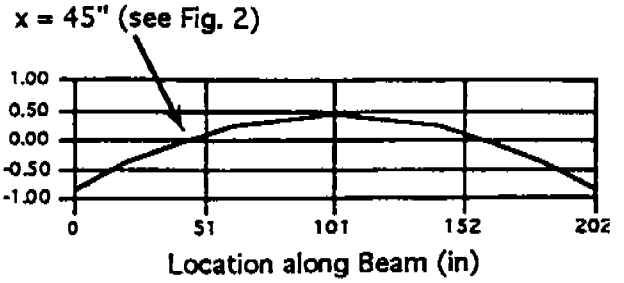

Figure 6
Normalized Moment for Clamped Longitudinal between Transverse Frames

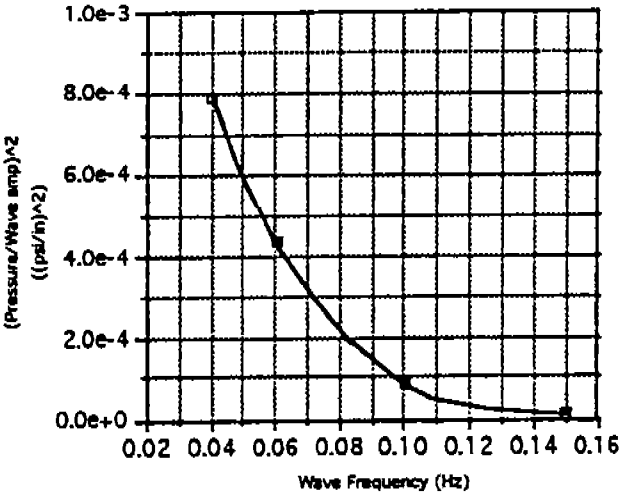

Figure 7
Panel Pressure transfer Function
(S5, Sta 6, WI 3)

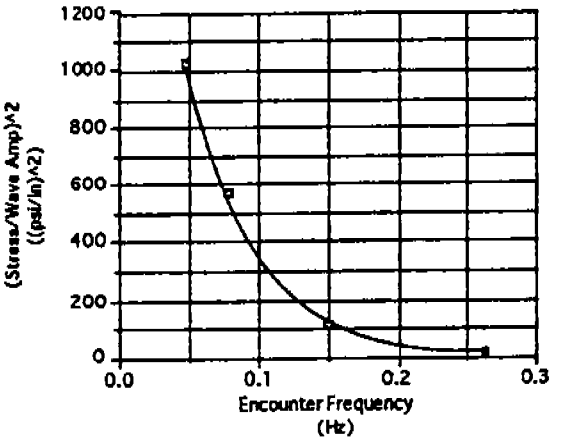

Figure 8
Web (Outer Edge) Stress Transfer Function for L32 at FR54 Due to Panel Pressure

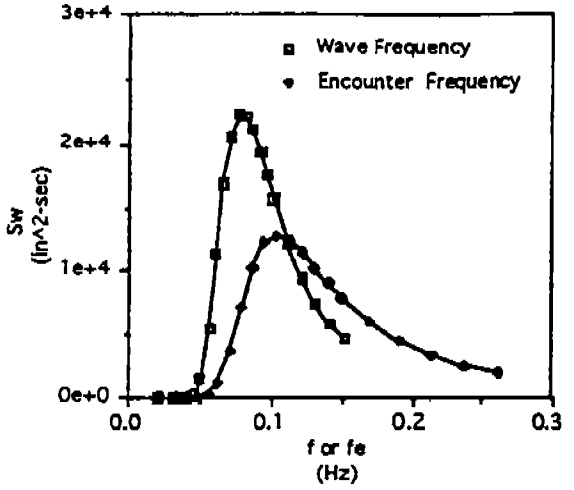

Figure 9
Wave and Encounter Frequency Spectra, Buoy 46002 at $H_{m_0} = 4.0$ m

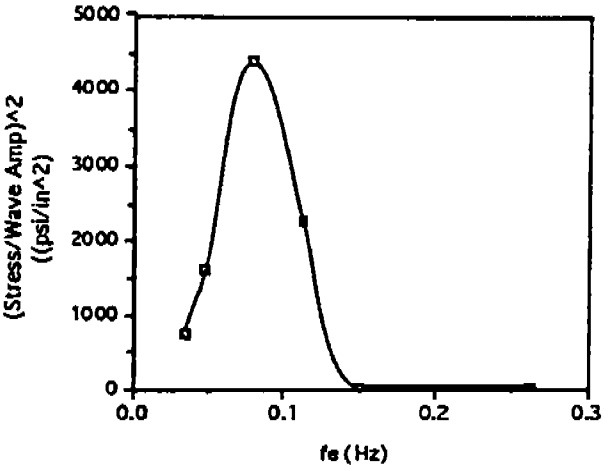

Figure 11
Transfer Function for Outer Web Stress in Longitudinal 32 Due to Hull Girder Bending

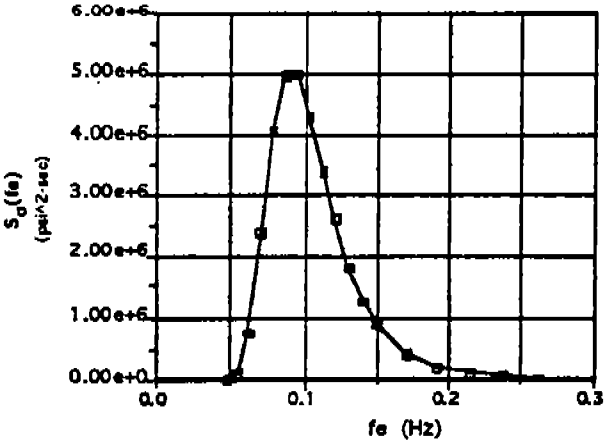

Figure 10
Response Spectrum, Sσ(fe), Buoy 46002 and $H_{m_0} = 4.0$ m

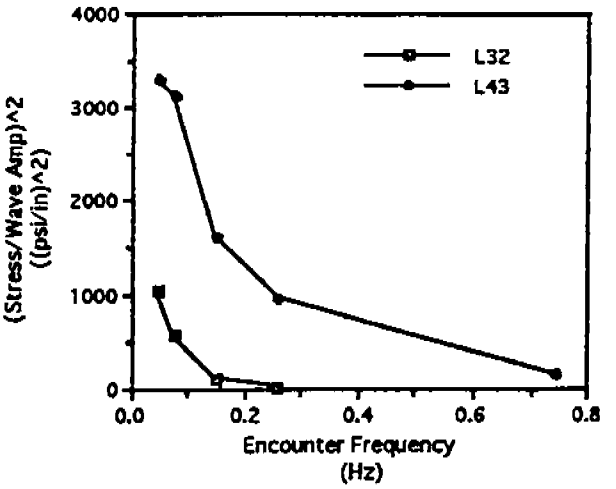

Figure 12
Stress Transfer Function L43 at FR54

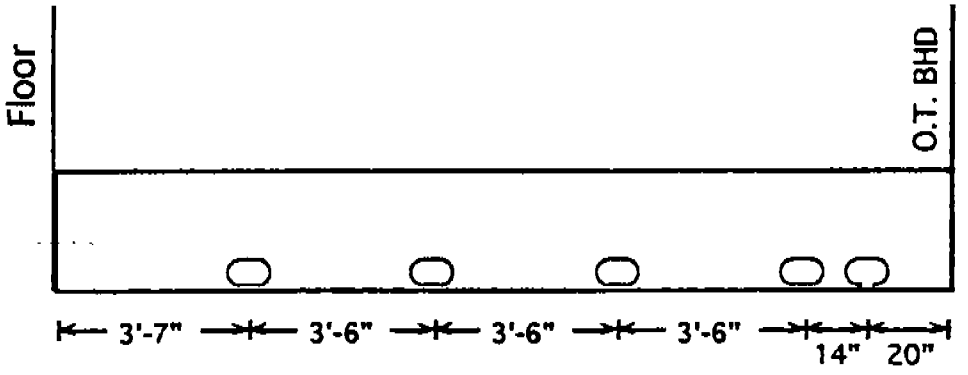

Figure 13
Bottom Longitudinal Geometry

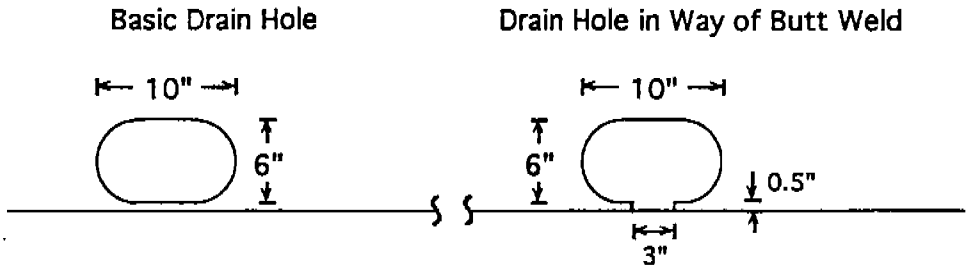

Figure 14
Bottom Longitudinal Drain Holes

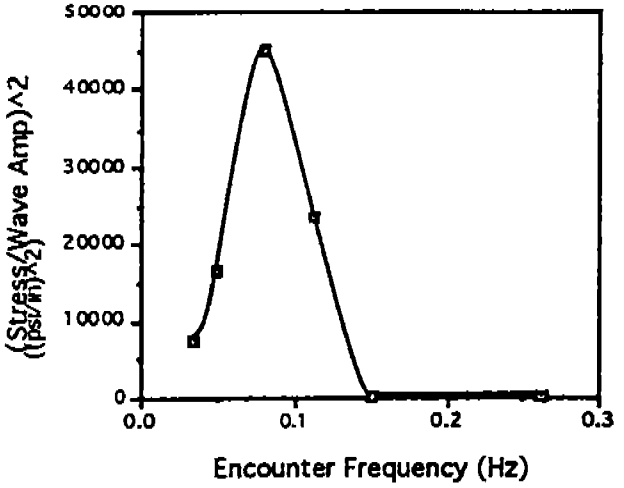

Figure 15
Stress Transfer Function for Bottom Longitudinal with SCF = 2.0

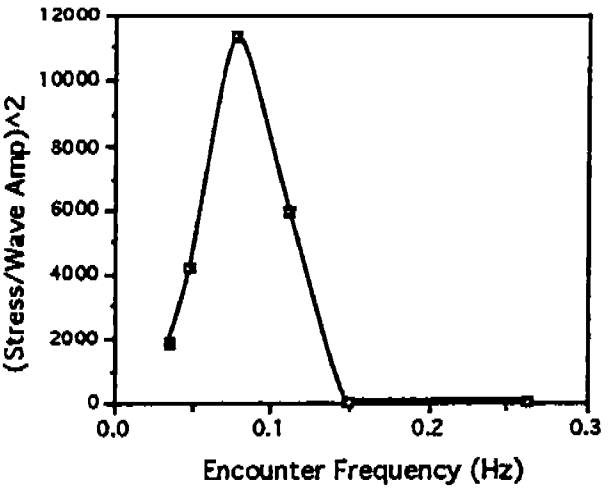

Figure 16
Bottom Longitudinal Butt-Weld Drain Hole Stress Transfer Function